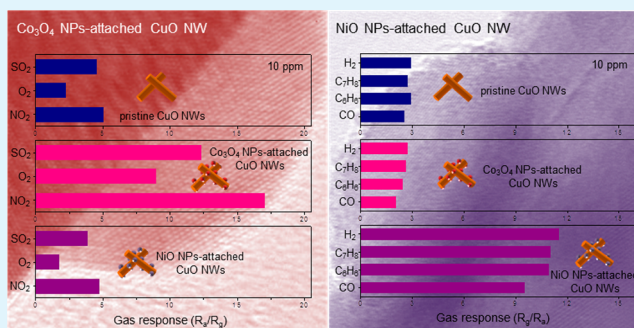# Remarkable Improvement of Gas-Sensing Abilities in p-type Oxide Nanowires by Local Modification of the Hole-Accumulation Layer

Sun-Woo Choi, Akash Katoch, Jae-Hun Kim, and Sang Sub Kim*

Department of Materials Science and Engineering, Inha University, Incheon 402-751, Republic of Korea

ABSTRACT: This paper proposes a method for improving the reducing or oxidizing gas-sensing abilities of p-type oxide nanowires (NWs) by locally modifying the hole-accumulation channel through the attachment of p-type nanoparticles (NPs) with different upper valence band levels. In this study, the sensing behaviors of p-CuO NWs functionalized with either p-NiO or p-Co$_3$O$_4$ NPs were investigated as a model materials system. The attachment of p-NiO NPs greatly improved the reducing gas-sensing performance of p-CuO NWs. In contrast, the p-Co$_3$O$_4$ NPs improved the oxidizing gas-sensing properties of p-CuO NWs. These results are associated with the local suppression/expansion of the hole-accumulation channel of p-CuO NWs along the radial direction due to hole flow between the NWs and NPs. The approach proposed in this study provides a guideline for fabricating sensitive chemical sensors based on p-CuO NWs.

KEYWORDS: gas sensor, sensing mechanism, p-type, oxide nanowires, electronic sensitization

1. INTRODUCTION

Oxide nanowires (NWs) have been explored for use as chemical sensors with both high response and reliability. Their large surface-to-volume ratio, high crystalline quality, self-heating nature, and large intrinsic resistance modulation because of their equivalent diameters to the Debye length are the key properties for realizing excellent chemical sensors.[1−4] Nevertheless, the sensing properties of NWs, such as the gas response, response and recovery times, which are the most important sensor parameters for actual sensor operations, require further improvement.

The approaches to improving the sensing abilities of NWs include doping, modification of the NW surface with the irradiation of electrons[5] or ions,[6,7] plasma exposure,[8,9] and the attachment of nanoparticles (NPs).[10−14] Among them, the attachment of NPs has been used most widely for the improvement thus far. The roles of NPs are classified as either "electronic sensitization" or "catalytic sensitization".[15] Catalytic sensitization is related to the spillover effect by the catalytic nature of the attached NPs.[16] Electronic sensitization is associated with the modification of the NW conduction channel originating from the flow of charge carriers between the NWs and NPs.

Although n-type NWs have been investigated intensively in terms of the sensing improvement and mechanism, much less attention has been focused on p-type NWs. The sensing mechanism of p-type NWs is different from that of n-type NWs; the sensing mechanism of the former is based on the modulation of resistance due mainly to changes in the hole-accumulation layer during the adsorption and desorption of gas molecules; the latter comes from changes in the electron-depletion layer.[17]

To the best of the authors' knowledge, few systematic studies aimed at improving the sensing properties of p-type NWs have examined the electronic sensitization caused solely by hole flow. This paper reports, for the first time, an approach to improving the sensing abilities of p-CuO NWs selectively for reducing or oxidizing gases by attaching p-type NPs with different upper valence band levels from p-CuO NWs. The related sensing mechanism is explained based on two different kinds of local radial modification of the hole-accumulation layer in p-CuO NWs that provide significant improvement in the reducing or oxidizing gas-sensing properties of p-CuO NWs. The approach reported in this study provides a valuable guideline for the fabrication of sensitive chemical sensors based on p-type NWs.

2. EXPERIMENTAL SECTION

Synthesis of Networked CuO NWs. Networked CuO NWs were grown on SiO$_2$ (200 nm thick)-grown Si (100) substrates by a thermal oxidation growth technique.[18] For the selective growth of CuO NWs, patterned interdigital electrodes (PIEs) were first prepared on Si substrates using a conventional photolithographic process. The details of the fabricated PIEs are as follows. The total number of electrode pads was 20. Each electrode pad was 1.05 mm long and 20 μm wide, and the gap between the neighboring electrode pads was 10 μm. For the fabrication of PIEs, negative photoresist (PR) (AZ 5214E, Clariant Industries Ltd., Seoul, Republic of Korea) with 2 μm thickness was spread on SiO$_2$/Si substrates using the spin-coating technique. The
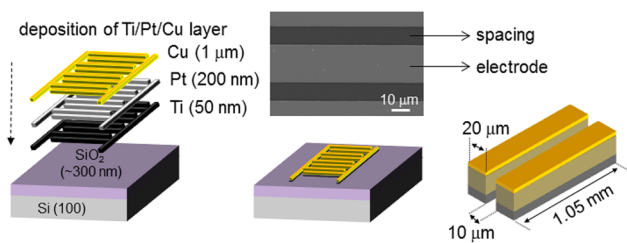
substrates covered with negative PR were exposed to ultraviolet (UV) radiation through photomask and then followed the developing process. The double layer consisting of Pt (200 nm)/Ti (50 nm) was deposited by the sputtering technique. The Ti layer was used to improve the adhesion between the Pt layer and the SiO_2/Si substrate. The Cu film with a thickness of 1.1 μm was deposited using the electron-beam evaporation technique. To remove the negative PR, the substrate was immersed into acetone with ultrasonification for 5 min. Then the lift-off process was carried out. In this way the electrode pad of a trilayer consisting of Cu (1.1 μm)/ Pt (200 nm)/Ti (50 nm) was fabricated. The Cu layer was used as the source of CuO nanowires. The PIE-fabricated Si substrate was heated to 500 °C for 4 h in air. During heat treatment, CuO nanowires grew by consuming the Cu layer.
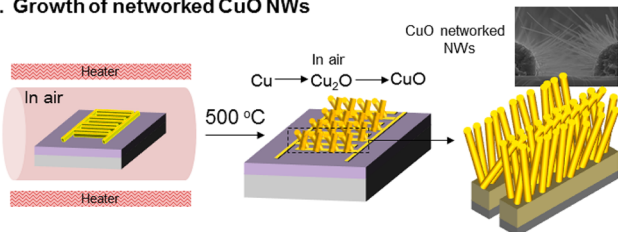
Attachment of Co_3O_4 and NiO NPs. To attach the p-Co_3O_4 and p-NiO NPs on the p-CuO NWs, the Co and Ni metal films were deposited directly on the networked CuO NWs by sputtering high-purity Co and Ni targets. The sputtering conditions used were as follows: the target-to-substrate distance was set to 10 cm; the base pressure of the chamber was $<4 \times 10^{-5}$ Torr; the deposition pressure was maintained at 10 mTorr with argon; the deposition time was 10 min with no intentional heating; and the thicknesses of the Co and Ni films were 10 and 5 nm, respectively. After heat treatment at 700 °C for 2 h in air, the discontinuous Co_3O_4 and NiO NPs were created on the surface of the p-CuO NWs. Figure 1 shows a schematic diagram of the overall process used to fabricate the NPs-attached CuO NWs sensors.

Materials Characterization and Sensing Measurement. The microstructure and structural phase of the samples were characterized by field-emission scanning electron microscopy (FE-SEM, Hitachi S-4200), transmission electron microscopy (TEM, Philips CM-200), and X-ray diffraction (XRD, Philips X'pert MRD). The compositional information was obtained by energy-dispersive X-ray spectroscopy (EDS, equipped in the FE-SEM system). The sensing performance of the NPs-attached CuO NWs for various oxidizing and reducing gases was investigated using a gas-sensing system. According to preliminary experiments, the optimal temperature for the best sensing performances was found to be 300 °C. Accordingly, all the sensing measurements were carried out at this temperature. The gas concentration was controlled by changing the dry air-balanced target gas and dry air mixing ratio using precise mass flow controllers. The gas response (R) for an oxidizing gas of the fabricated sensors was evaluated by the ratio R_a/R_g, where R_a and R_g are the resistances in the absence and presence of the target gas, respectively. For reducing gases, R_g/R_a was used as the gas response.

3. RESULTS AND DISCUSSION

The microstructures of the NPs-attached CuO NWs were investigated. Figure 2a shows a representative cross-sectional FE-SEM image of the networked CuO NWs, which played the

Figure 2. (a) A cross-sectional FE-SEM image of p-CuO NWs grown on a SiO_2/Si substrate. (b) A high-magnification FE-SEM image of p-CuO NWs functionalized with Co_3O_4 NPs. (c) A high-resolution TEM image taken from a region of p-Co_3O_4 NP-attached p-CuO NW. (d) EDS elemental line profiles for Co, Cu, and O. Microstructures of NiO NP-attached CuO NWs: (e) FE-SEM image, (f) low-magnification TEM image, (g) high-resolution lattice image taken from the NiO-CuO interface, and (h) EDS elemental line profiles of Ni, Cu, and O around a NiO NP.

I. Fabrication of patterned interdigital electrode

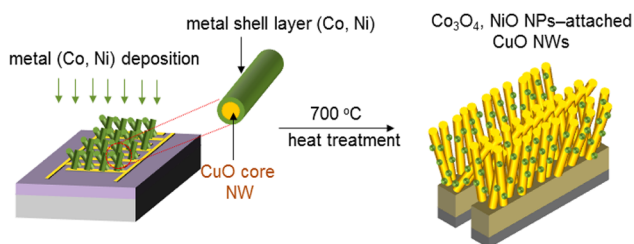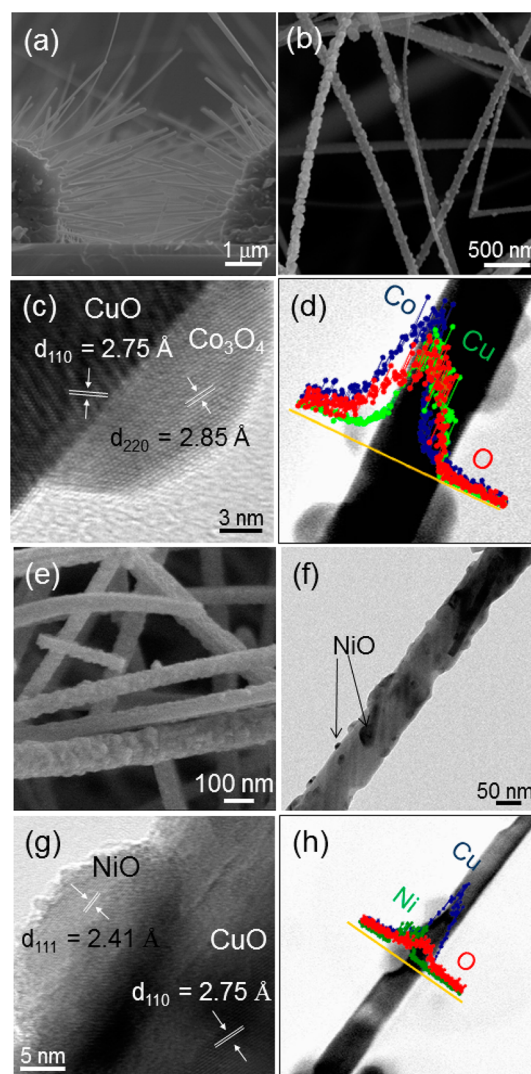**II. Growth of networked CuO NWs**

III. Attachment of Co_3O_4 and NiO NPs

Figure 1. Schematic illustration of the overall process used in this study for preparing NPs-attached CuO NWs sensors.

role of sensor platforms. The CuO NWs grown locally on the adjacent PIEs touched each other, forming junctions in the middle of the spacing between the PIEs. The mean diameter of the CuO NWs was ~70 nm, and TEM (data not shown) showed the single-crystalline nature of the CuO NWs without considerable dislocations and stacking faults. This networked propensity of CuO NWs is basically the same as the result[19] obtained for SnO_2 NWs sensors reported by the current authors.

On these networked CuO NWs, Co_3O_4 NPs were attached. As shown in Figure 2b, discrete NPs were attached to the surface of CuO NWs, which were identified as Co_3O_4 by high-resolution TEM and XRD. The high-resolution TEM image shown in Figure 2c showed that the interface between the Co_3O_4 NP and the CuO NW was very abrupt, suggesting that no considerable interdiffusion had taken place. The lattice fringe separated by 2.85 Å corresponded to the interplanar distance of the Co_3O_4 (220) planes. The lattice fringe separated by 2.75 Å was assigned to the CuO (110) planes. The composition of the Co_3O_4 NPs-attached CuO NWs was characterized by EDS, and the result is shown in Figure 2d, confirming the presence of Co, Cu, and O. Figure 2e shows the typical microstructures of NiO NPs-attached CuO NWs. The NiO NPs are attached uniformly to the CuO NWs. The lattice fringes shown in Figure 2g and the EDS line profiles in Figure 2h revealed the successful attachment of NiO NPs on the CuO NWs. The structural phases of the pristine, Co_3O_4 or NiO NPs-attached CuO NWs were examined by XRD, and the results are shown in Figure 3. The XRD peaks from the Co_3O_4 (JCPDS
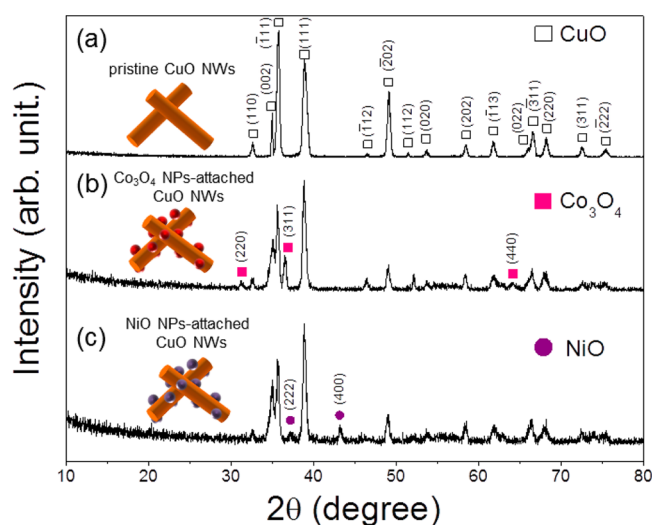

Figure 3. X-ray θ-2θ diffraction patterns obtained for (a) pure CuO, (b) Co_3O_4, and (c) NiO NPs-attached p-CuO NWs.

No. 78−1970) and NiO (JCPDS No. 89−5881) phases are evident with the CuO phase, again demonstrating the successful synthesis of the NPs-attached CuO NWs.

The sensing properties of the NPs-attached CuO NWs were investigated for oxidizing gases, NO_2, O_2, and SO_2, with gas concentrations ranging from 1 to 10 ppm. As shown in Figure 4a, all the sensors exhibited p-type sensing behavior. That is, the resistance decreased in the presence of the oxidizing gases tested and retained its original value in the absence of those gases. For comparison, Figure 4b summarizes the responses of the sensors for 10 ppm gases. The attachment of Co_3O_4 NPs improved significantly the responses of the pristine CuO NWs
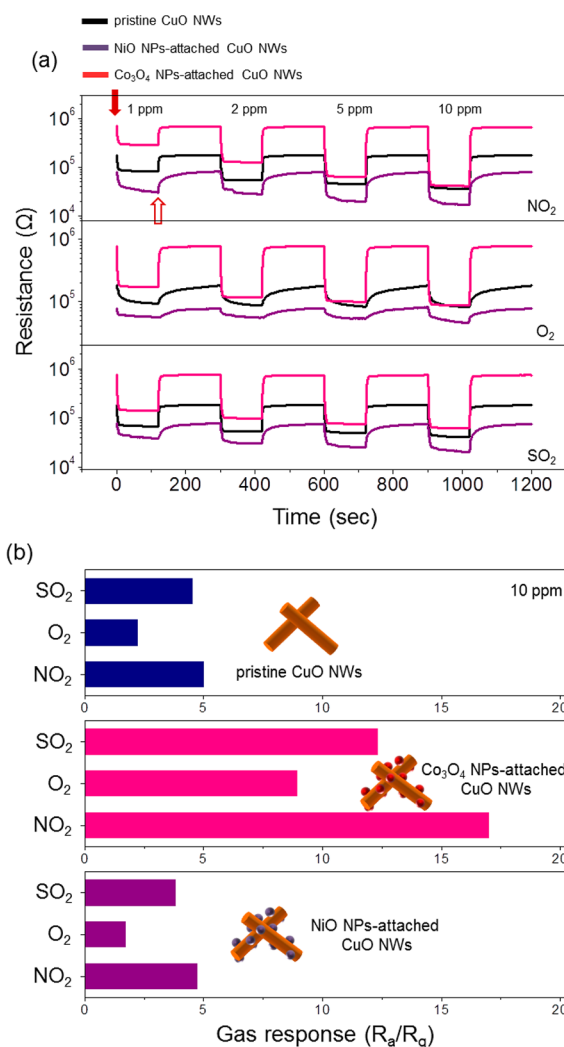

Figure 4. (a) Response curves for pristine CuO NWs, Co_3O_4, and NiO NPs-attached CuO NWs for oxidizing gases such as NO_2, O_2, and SO_2 at 300 °C. (b) Summary of responses to 10 ppm oxidizing gases.

to the oxidizing gases. In sharp contrast, the NiO NPs did not have a noticeable effect on the sensing properties of CuO NWs.

The sensing properties of the NPs-attached CuO NWs for reducing gases, CO, C_6H_6, C_7H_8, and H_2 ranging from 1 to 10 ppm, were investigated, and the results are shown in Figure 5. The sensor resistance increased with increasing supply of the reducing gases and returned to its initial value reversibly after stopping the gases and exposing them to dry air. This is also the typical sensing behavior of p-type oxide semiconductors under a reducing-gas atmosphere. The responses summarized in Figure 5b show the effectiveness of each NP more clearly. The NiO NPs improved considerably the reducing gas-sensing properties of the pristine CuO NWs. On the other hand, the attachment of Co_3O_4 NPs had no significant effect on the reducing gas-sensing properties of the CuO NWs. It is of note that the response of pristine p-type CuO NWs is lower for oxidizing gases in comparison to n-type SnO_2 nanowires that are most widely used sensor materials and show the response of 90−130.[20] The low response of p-type CuO NWs is likely to be originated from the intrinsic p-type sensing mechanism. In n-type semiconductors, adsorbed oxidizing gaseous species extract the electrons lying in their conduction band. In contrast, in p-type semiconductors oxidizing species extract the electrons
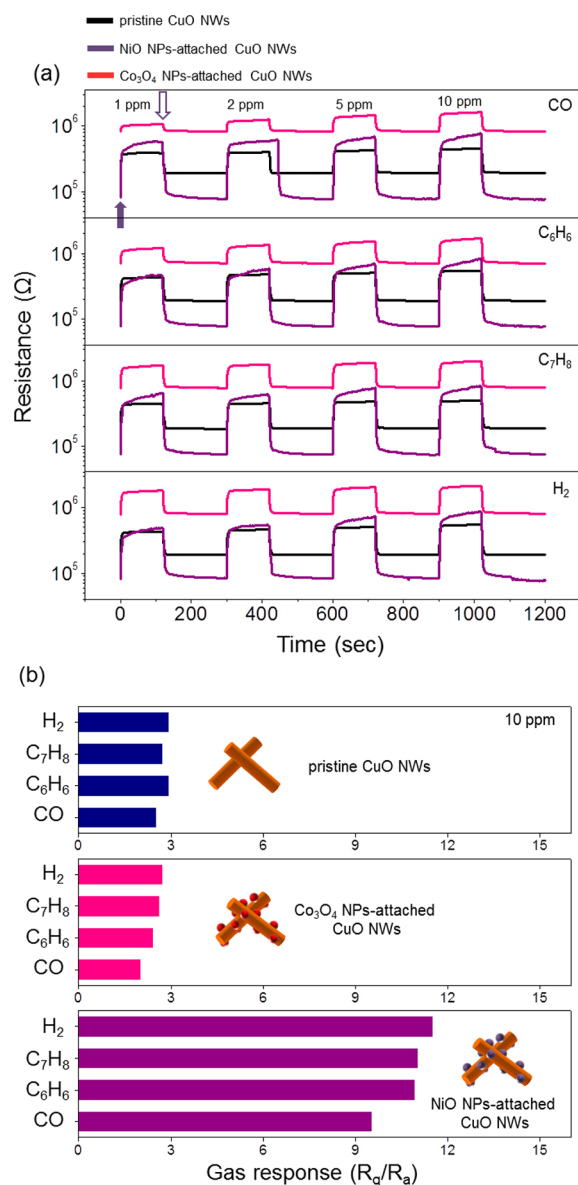
Figure 5. (a) Resistance curves obtained when p-Cr$_2$O$_3$ NPs-functionalized n-SnO$_2$ NWs were exposed to various oxidizing gases, such as SO$_2$, O$_2$, and NO$_2$ at 300 °C. (b) Summary of gas responses to 10 ppm of each gas.

Figure 6. Schematic illustration showing the gas-sensing mechanisms: (a) change of hole-accumulation layer of a pristine CuO NW upon exposure to reducing or oxidizing gases; (b) suppression of hole-accumulation layer by hole flow from CuO NWs to Co$_3$O$_4$ NPs, and the band structure of the CuO−Co$_3$O$_4$ p−p interface; (c) change of hole-accumulation layer of Co$_3$O$_4$ NPs-attached CuO NWs upon exposure to reducing or oxidizing gases; (d) expansion of hole-accumulation layer by hole flow from NiO NPs to CuO NWs, and the band structure of the CuO−NiO p−p interface; (e) change of hole-accumulation layer of NiO NPs-attached CuO NWs upon exposure to reducing or oxidizing gases.

in their valence band, which requires more energy than the case of taking electrons in the conduction band. This can be the reason for the lower response of p-type semiconductors including CuO for oxidizing gases. However, pristine CuO NW capability of detecting reducing gases is somewhat superior or at least comparable to that of SnO$_2$ nanowires.[20]

The attachment of proper oxide NPs to p-type NWs resulted in improved NWs sensing for either reducing or oxidizing gases. The mechanism for this behavior can be explained based on the electronic sensitization by hole flow between the NPs and NWs. In Figure 6a, for pristine p-CuO NWs in air, oxygen molecules adsorb on the NWs, extracting electrons in the valence band of the p-CuO NWs, consequently creating holes. These additionally created holes will be present beneath the surface of p-CuO NWs, forming a hole-accumulation layer. The width of the hole-accumulation layer along the radial direction was estimated using eq 1
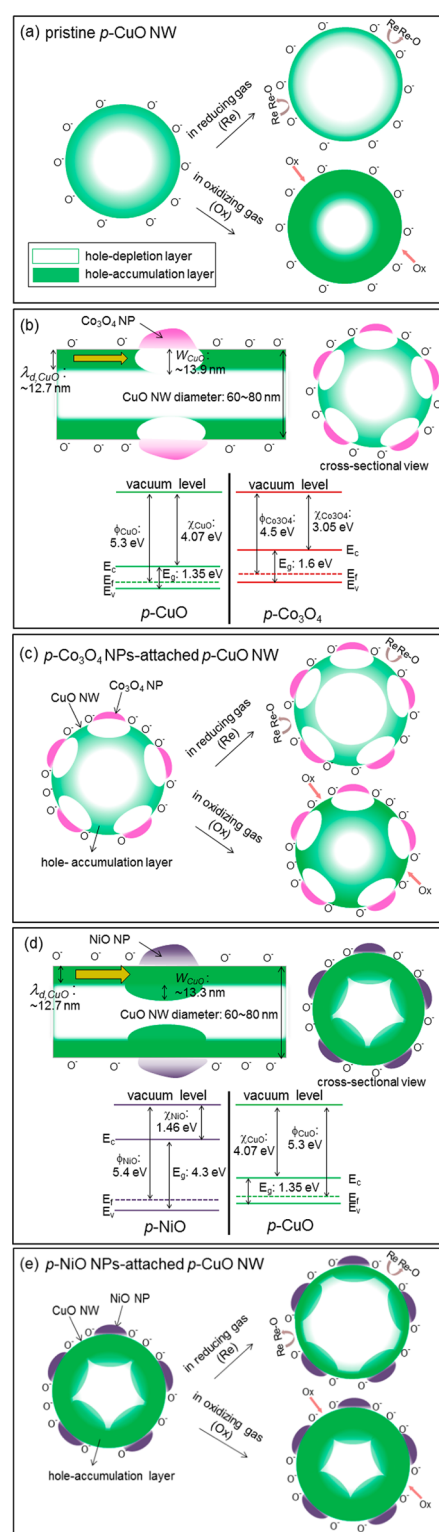
$$\lambda_d = \left[\frac{2\varepsilon \text{CuO} \phi}{q^2 N_{\text{CuO}}} \right]^{1/2} \qquad (1)$$

where ϕ is the height of the potential barrier established by oxygen adsorption, ε_{CuO} is the permittivity of CuO, N_{CuO} is the hole concentration in CuO, and q is the charge of an electron ($= 1.6 \times 10^{-19}$ C). With values of $N_{\text{CuO}} \approx 10^{19}$ cm^{-3} at room temperature, $\varepsilon_{\text{CuO}} \approx 25$, and $\phi \approx 0.59$ eV,[21,22] the calculated width, λ_d, was ~12.7 nm. When an oxidizing gas was supplied, the hole-accumulation layer will expand because oxidizing gas molecules will further extract the valence-band electrons, corresponding to an expansion of the electrical transport channel, eventually leading to a decrease in resistivity. On the other hand, when a reducing gas is supplied, the adsorbed oxygen species will evaporate from the NW surface because the reducing gas molecules interact with them and form volatile molecules. Upon the application of this process, the captured electrons will return to the valence band, resulting in electron–hole compensation and eventually suppressing the hole-accumulation layer. This suppression results in an increase in resistance when a reducing gas is supplied.

In contrast to this regular modulation of the hole-accumulation layer occurring in the pure p-CuO NWs, the attachment of p-type NPs will result in additional expansion or suppression of the hole-accumulation layer, as illustrated schematically in Figure 6b,d. When p-type NPs such as Co$_3$O$_4$ are attached to the p-CuO NWs, the upper valence band level of Co$_3$O$_4$ is higher than that of p-CuO NWs, and hole flow takes place from the NPs to NWs. This will make the hole-accumulation layer in p-CuO NWs locally narrower. The additional suppression can be calculated using eq 2.

$$W_{\text{CuO}} = \left[\frac{2\varepsilon_{\text{CuO}}\varepsilon_{\text{Co3O4}} N_{\text{Co3O4}} V_0}{q N_{\text{CuO}}(\varepsilon_{\text{CuO}} N_{\text{CuO}} + \varepsilon_{\text{Co3O4}} N_{\text{Co3O4}})} \right]^{1/2} \qquad (2)$$

where V_0 ($= 0.8$ eV) is the contact potential difference between Co$_3$O$_4$ and CuO, $\varepsilon_{\text{Co3O4}}$ is the permittivity of CO$_3$O$_4$, N_{Co3O4} and N_{CuO} are the hole concentrations in the NPs and NWs, respectively ($N_{\text{Co3O4}} = 4.5 \times 10^{19}$ and $N_{\text{CuO}} = 10^{19}$ cm^{-3}).[23,24] The calculated W_{CuO} was ~13.9 nm. In this state, as shown in Figure 6b, the supply of oxidizing gases will expand the locally suppressed hole-accumulation layer, providing a greater change in resistance of the p-CuO NWs, which is why the attachment of Co$_3$O$_4$ NPs greatly improved the oxidizing gas-sensing performance of p-CuO NWs. In contrast, when reducing gases are supplied, the already locally suppressed hole-accumulation layer is marginally suppressed, being indicative of the small resistance modulation.

When p-type NPs like NiO, whose upper valence band level is lower than that of p-CuO NWs, are attached to p-CuO NWs, holes will flow from the NWs to the NPs. This will locally widen the hole-accumulation layer in p-CuO NWs. The expansion width was calculated using eq 3.

$$W_{\text{CuO}} = \left[\frac{2\varepsilon_{\text{CuO}}\varepsilon_{\text{NiO}} N_{\text{NiO}} V_0}{q N_{\text{CuO}}(\varepsilon_{\text{CuO}} N_{\text{CuO}} + \varepsilon_{\text{NiO}} N_{\text{NiO}})} \right]^{1/2} \qquad (3)$$

where V_0 ($= 0.1$ eV) is the contact potential difference between NiO and CuO, ε_{NiO} is the permittivity of NiO, N_{NiO} and N_{CuO} are the hole concentrations in the NPs and NWs, respectively ($N_{\text{NiO}} = 3.13 \times 10^{18}$ and $N_{\text{CuO}} = 10^{19}$ cm^{-3}).[23,25] The calculated W_{CuO} was ~13.3 nm, as shown in Figure 6d. In this case,

reducing gases will make more pronounced resistance modulation compared to oxidizing gases. The parameters used for calculation of Debye lengths and space charge layers in this study is summarized in Table 1. It should be mentioned

Table 1. Parameters Used for Calculation of Debye Lengths and Space Charge Layers

materials	work function (eV)	electron affinity (eV)	permittivity	hole concentration (cm^{-3})
CuO	5.3[a]	4.07[b]	25[c]	10^{19} [d]
Co$_3$O$_4$	4.5[e]	3.05[f]	12.9[g]	4.5 × 10^{19} [h]
NiO	5.4[i]	1.46[j]	8.86[k]	3.13 × 10^{18} [j]

[a]Reference 26. [b]Reference 27. [c]Reference 21. [d]Reference 23 [e]Reference 28. [f]Reference 29. [g]Reference 30. [h]Reference 24 [i]Reference 31. [j]Reference 32. [k]Reference 33. [j]Reference 25

here that all the values were calculated on the basis of room-temperature parameters, not ones at 300 °C. However, in spite of a slight difference from the exact value, the sensing mechanism proposed here is still effective in explanation of the observed sensing results.

In this work, the attachment of NPs on the surface of CuO NWs was achieved by the sputtering technique, which is a line-of-sight deposition process. This means that NPs were created preferentially on one side of CuO NWs. In addition, it is likely that NPs were less created on CuO NWs existing at the bottom of the networked NWs mat. However, the model proposed here is still valid though the effect of radial modulation of hole-accumulation layer is weakened due to the nonuniform attachment of NPs. It is also of note that the population density of NPs needs to be optimized to obtain the best sensing properties. Specifically, either smaller or larger amounts of NPs than an optimized one will not be effective. Detailed investigations need to be performed at a later stage of study on the sensing properties in relation to the population density of NPs.

4. CONCLUSIONS

This paper reported an approach for improving the reducing or oxidizing gas-sensing abilities of p-type oxide NWs by modifying the hole-accumulation layer by attaching p-type NPs based on hole flow. p-NiO NPs greatly improved the reducing gas-sensing performance of p-CuO NWs. On the other hand, the p-Co$_3$O$_4$ NPs improved the oxidizing gas-sensing properties of the p-CuO NWs. This selective sensing improvement is related to the local suppression/expansion of the hole-accumulation channel of p-CuO NWs due to hole flow between the NWs and NPs caused by the difference in the upper valence band level. The results provide useful guidelines to the fabrication of sensitive chemical sensors using p-CuO NWs.

■ AUTHOR INFORMATION

Corresponding Author
*E-mail: sangsub@inha.ac.kr.

Author Contributions
S.S.K. conceived the study, designed the experiments, and prepared the manuscript. S.-W.C., A.K., and J.-H.K. performed the experiments. All authors have given approval to the final version of the manuscript.

■ REFERENCES

(1) Law, M.; Kind, H.; Messer, B.; Kim, F.; Yang, P. Photochemical Sensing of NO$_2$ with SnO$_2$ Nanoribbon Nanosensors at Room Temperature. *Angew. Chem., Int. Ed.* **2002**, *41*, 2405−2408.

(2) Kolmakov, A.; Moskovits, M. Metal Oxide Nano-Crystals for Gas Sensing. *Annu. Rev. Mater. Res.* **2004**, *34*, 151−180.

(3) Prades, J. D.; Jimenez-Diaz, R.; Hernandez-Ramirez, F.; Barth, S.; Cirera, A.; Romano-Rodriguez, A.; Mathur, S.; Morante, J. R. Utlralow Power Consumption Gas Sensors Based on Self-Heated Individual Nanowires. *Appl. Phys. Lett.* **2008**, *93*, 123110.

(4) Wang, C.; Yin, L.; Zhang, L.; Xiang, D.; Gao, R. Metal Oxide Gas Sensors: Sensitivity and Influencing Factors. *Sensors* **2010**, *10*, 2088−2106.

(5) Dhawale, D. S.; Salunkhe, R. R.; Fulari, V. J.; Rath, M. C.; Sawant, S. N.; Lokhande, C. D. Liquefied Petroleum Gas (LPG) Sensing Performance of Electron Beam Irradiated Chemically Deposited TiO$_2$ Thin Films. *Sens. Actuators, B* **2009**, *141*, 58−64.

(6) Liao, L.; Lu, H. B.; Li, J. C.; Liu, C.; Fu, D. J. The Sensitivity of Gas Sensor Based on Single ZnO Nanowire Modulated by Helium Ion Radiation. *Appl. Phys. Lett.* **2007**, *91*, 173110.

(7) Katoch, A.; Sun, G.-J.; Choi, S.-W.; Hishita, S.; Kulish, V. V.; Wu, P.; Kim, S. S. Acceptor-Compensated Charge Transport and Surface Chemical Reactions in Au-Implanted SnO$_2$ Nanowires. *Sci. Rep.* **2014**, *4*, 4622.

(8) Pan, J.; Ganesan, R.; Shen, H.; Mathur, S. Plasma-Modified SnO$_2$ Nanowires for Enhanced Gas Sensing. *J. Phys. Chem. C* **2010**, *114*, 8245−8250.

(9) Kim, H. W.; Choi, S.-W.; Katoch, A.; Kim, S. S. Enhanced Sensing Performances of Networked SnO$_2$ Nanowires by Surface Modification with Atmospheric Ar-O$_2$ Plasma. *Sens. Actuators, B* **2013**, *177*, 654−658.

(10) Kuang, Q.; Lao, C.-S.; Li, Z.; Liu, Y.-Z.; Xie, Z.-X.; Zheng, L.-S.; Wang, Z. L. Enhancing the Photon- and Gas-Sensing Properties of a Single SnO$_2$ Nanowire Based Nanodevice by Nanoparticle Surface Functionalization. *J. Phys. Chem. C* **2008**, *112*, 11539−11544.

(11) Choi, S.-W.; Jung, S.-H.; Kim, S. S. Functionalization of Selectively Grown Networked SnO$_2$ Nanowires with Pd Nanodots by γ-ray Radiolysis. *Nanotechnology* **2011**, *22*, 225501.

(12) Na, C. W.; Woo, H.-S.; Lee, J.-H. Design of Highly Sensitive Volatile Organic Compound Sensors by Controlling NiO Loading on ZnO Nanowire Networks. *RSC Adv.* **2012**, *2*, 414−417.

(13) Mashock, M.; Yu, K.; Cui, S.; Mao, S.; Lu, G.; Chen, J. Modulating Gas Sensing Properties of CuO Nanowires through Creation of Discrete Nanosized p-n Junctions on Their Surfaces. *ACS Appl. Mater. Interfaces* **2012**, *4*, 4192−4199.

(14) Na, C. W.; Park, S.-Y.; Chung, J.-H.; Lee, J.-H. Transformation of ZnO Nanobelts into Single-Crystalline Mn$_3$O$_4$ Nanowires. *ACS Appl. Mater. Interfaces* **2012**, *4*, 6565−6572.

(15) Franke, M. E.; Koplin, T. J.; Simon, U. Metal and Metal Oxide Nanoparticles in Chemiresistors: Dose the Nanoscale Matter? *Small* **2006**, *2*, 36−50.

(16) Baik, J. M.; Kim, M. H.; Larson, C.; Yavuz, C. T.; Stucky, G. D.; Wodtke, A. M.; Moskovits, M. Pd-Sensitized Single Vanadium Oxide Nanowires: Highly Responsive Hydrogen Sensing Based on the Metal-Insulator Transition. *Nano Lett.* **2009**, *9*, 3980−3984.

(17) Kim, H.-J.; Lee, J.-H. Highly Sensitive and Selective Gas Sensors Using p-Type Oxide Semiconductors: Overview. *Sens. Actuators, B* **2014**, *192*, 607−627.

(18) Jiang, X.; Herricks, T.; Xia, Y. CuO Nanowires Can Be Synthesized by Heating Copper Substrates in Air. *Nano Lett.* **2002**, *2*, 1333−1338.

(19) Park, J. Y.; Choi, S.-W.; Kim, S. S. Junction-Tuned SnO$_2$ Nanowires and Their Sensing Properties. *J. Phys. Chem. C* **2011**, *115*, 12774−12781.

(20) Choi, S.-W.; Katoch, A.; Kim, J.-H; Kim, S. S. Prominent Reducing Gas-Sensing Performances of n-SnO$_2$ Nanowires by Local Creation of p-n Heterojunctions by Functionalization with p-Cr$_2$O$_3$ Nanoparticles. *ACS Appl. Mater. Interfaces* **2014**, *6*, 17723−17729.

(21) Sarkar, S.; Jana, P. K.; Chaudhuri, B. K.; Sakata, H. Copper (II) Oxide as a Giant Dielectric Materials. *Appl. Phys. Lett.* **2006**, *89*, 212905.

(22) Li, D.; Hu, J.; Wu, R.; Lu, J. G. Conductometric Chemical Sensor Based on Individual CuO Nanowires. *Nanotechnology* **2010**, *21*, 485502.

(23) Samokhvalov, A. A.; Viglin, N. A.; Gizhevskiĭ, B. A.; Loshkareva, N. N.; Osipov, V. V.; Solin, N. I.; Sukhorukov, Y. P. Low-Mobility Charge Carriers in CuO. *J. Exp. Theor. Phys.* **1993**, *76*, 463−468.

(24) Chougule, M. A.; Pawar, S. G.; Godse, P. R.; Sakhare, R. D.; Sen, S.; Patil, V. B. Sol-Gel Derived Co$_3$O$_4$ Thin Films: Effect of Annealing on Structural, Morphological and Optoelectronic Properties. *J. Mater. Sci.: Mater. Electron.* **2012**, *23*, 772−778.

(25) Chen, H.-L.; Lu, Y.-M.; Hwang, W.-S. Characterization of Sputtered NiO Thin Fims. *Surf. Coat. Technol.* **2005**, *198*, 138−142.

(26) Mangamma, G.; Jayaraman, V.; Gnanasekaran, T.; Periaswami, G. Effects of Silica Additions on H$_2$S Sensing Properties of CuO-SnO$_2$ Sensors. *Sens. Actuators, B* **1998**, *53*, 133−139.

(27) Koffyberg, B. G.; Benko, F. A. A Photoelectrochemical Determination of the Position of the Conduction and Valence Band Edges of p-Type CuO. *J. Appl. Phys.* **1982**, *53*, 1173−1177.

(28) Varghese, B.; Mukherjee, B.; Karthik, K. R. G.; Jinesh, K. B.; Mhaisalkar, S. G. Electrical and Photoresponse Properties of Co$_3$O$_4$ Nanowires. *J. Appl. Phys.* **2012**, *111*, 104306.

(29) Miura, A.; Uraoka, Y.; Fuyuki, T.; Yoshii, S.; Yamashit, I. Floating Nanodot Gate Memory Fabrication with Biomineralized Nanodot as Charge Storage Node. *J. Appl. Phys.* **2008**, *103*, 074503.

(30) Cheng, C.-S.; Serizawa, M.; Sakata, H.; Hirayama, T. Electrical Conductivity of Co$_3$O$_4$ films prepared by chemical vapour deposition. *Mater. Chem. Phys.* **1998**, *53*, 225−230.

(31) Irwin, M. D.; Bruce Buchholz, D.; Hains, A. W.; Chang, R. P. H.; Marks, T. J. p-Type Semiconducting Nickel Oxide as an Efficiency-Enhancing Anode Interfacial Layer in Polymer Bulk-Heterojunction Solar Cells. *Proc. Natl. Acad. Sci. U. S. A.* **2008**, *105*, 2783−2787.

(32) Wu, H.; Wang, L.-S. A Study of Nickel Monoxide (NiO), Nickel Dioxide (ONiO), and Ni(O$_2$) Complex by Anion Photoelectron Spectroscopy. *J. Chem. Phys.* **1997**, *107*, 16−21.

(33) Choi, J. S.; Kim, J.-S.; Hwang, I. R.; Hong, S. H.; Jeon, S. H.; Kang, S.-O.; Park, B. H.; Kim, D. C.; Lee, M. J.; Seo, S. Different Resistance Switching Behaviors of NiO Films Deposited on Pt and SrRuO$_3$ Electrodes. *Appl. Phys. Lett.* **2009**, *95*, 022109.